Influence of wheel diameter difference on surface damage for heavy-haul locomotive wheels: Measurements and simulations

Influence of wheel diameter difference on surface damage for heavy-haul locomotive wheels: Measurements and simulations

Kaikai Lyu [1], Kaiyun Wang [1,*], Liang Ling [1], Yu Sun [2], Zhiyong Shi [3], Wanming Zhai [1]

[1] State Key Laboratory of Traction Power, Southwest Jiaotong University, Chengdu, Sichuan, China

[2] College of Transportation Science and Engineering, Nanjing Tech University, Nanjing, Jiangsu, China

[3] Department of Industrial Engineering, University of Florence, Florence, Florence, Italy

Abstract

Wheel surface damage has a significant impact on the maintenance cost and operation efficiency, in return, the wheel maintenance is also closely related to its surface condition. Based on a practical case occurred on heavy-haul locomotive, the wheel surface damage caused by wheel diameter difference (WDD) has been investigated by means of field observation, statistical analysis, and numerical simulation. By measuring the wheel wear, wheel diameter and observing the crack characteristic, the initial WDD due to unqualified maintenance is confirmed to be the main cause of wheel surface damage. The serious crack and partial wear are both developed quickly on a certain wheelset with large initial WDD, which always occurred on the wheel with smaller diameter, whereas the other side wheel is in well condition. The cracks are mainly located on a band of 65mm-120mm from flange back (outside of wheel centre). According to the numerical simulation, the initial WDD and unworn profiles will not increase the cracks significantly, especially in the field side of wheel tread. However, in conditions of measured worn profiles and WDD, the cracks in field side of wheel tread are increased obviously. It is to say that, the initial WDD first causes the wheel partial wear, and the worn profiles combined with the WDD further exacerbate wheel surface cracks.

Keywords: wheel diameter difference; heavy-haul locomotive; wheel partial wear; damage position; wheel profiles.

1. Introduction

Chinese heavy-haul industry is developing rapidly in recent years, the traction tonnage, length of train formation and locomotive power are both made a great promotion. In this process, some intractable issues are exposed, such as wheel surface damage. Owing to advanced detection technology and timely wheel turning, catastrophic accidents were not reported due to wheel surface damage, such as derailment mentioned in [1–4], but frequently wheel turning greatly shortens service life of wheelset and leads to significant operational disturbances. The problem of wheel surface damage especially caused by rolling contact fatigue (RCF) was overviewed in [5–8], which give a summary of its initiation, propagation, influence factors and prediction models. Predicting wheel surface damage is a fairly tough problem because the wheel experiences a full range of curves, slopes, running speeds, and even traction and braking forces for locomotive. In several proposed models for RCF [9–12], the shakedown map [13] and damage function [14] are commonly used due to its simplicity and relatively accurate. The shakedown map uses material failure mechanism under repeated loading cycles to predicted crack initiation. And the damage function further considers the competitive relation of wheel surface wear and RCF, as well as the influence of liquid trapped into the cracks [15].

Although the mechanism of wheel surface damage is gradually understood by the efforts of researchers, there is still a long way to solve the worldwide difficulty completely. Luo et al. [16] studied an abnormal surface damage happened on locomotive wheels caused by wheelset longitudinal vibration, some suggestions for optimizing suspension parameters to extending wheel life are proposed. Stichel et al. [17] compared the simulations and real behaviour of circumferential

RCF on wheel tread aiming three different vehicles, and the damage function shows a slightly better correlation to the experiences of RCF. The mitigating actions and its effect for wheel RCF are illustrated in [18], which mainly included locomotive-mounted lubrication, increasing wear thereby wear off incipient cracks, and matching wheel and rail profiles. Many researchers have focused on optimizing wheel and rail profiles to mitigate the wheel RCF [19–22], and its effects are needed to be further verified. Spangenberg et al. [23] discussed the effects of RCF mitigation measures (changing suspension stiffness and rail profile design) on wheel wear and rail fatigue. Improving the fatigue resistance of wheel materials is another worthwhile effort, which is discussed in [24–26]. It is found from the existing research of wheel RCF, the first step of investigation of wheel surface damage is to make an accurate identification of its main causes, the means include field observation of damage features [27], statistical analyses of occurring location [28,29], and surveying operation and maintenance status of the vehicle or locomotive [18,30]. Associating the observed crack features with the running conditions of the vehicle is essential for the mechanism and mitigation measures of wheel surface damage.

This paper focuses on a practical case about wheel abnormal surface damage caused by unqualified maintenance (main the initial WDD), which is occurred on locomotive widely used in Chinese heavy-haul railway. The features of wheel surface crack and wear are exhibited in detail based on field observations and measurements. And the mechanism of wheel surface damage due to WDD is investigated by statistical analysis and numerical simulation. The current study might lead to a better understanding of the wheel surface damage related to wheel maintenance, and the presented ideas and suggestions are expected to be valuable for promoting further research on mitigating this

problem.

2. Field observation and measurement of wheel tread

The studied locomotive is widely used in Chinese railway, and its wheels rarely suffer tread damage on most operational lines from the feedback of its manufacturer. However, severe wheel surface damage is still reported from a locomotive depot, which leads to a sharp decrease of wheel life because of frequently wheel lathe turning. The field observations and measurements were first carried out for identifying its main causes, which include the damage features, wheel profile shape and other key parameters.

2.1 Damage features

The typical observed wheel surface damage is shown in Fig. 1. Surface deterioration is clearly observed around the wheel circumference, seen Fig. 1(a), which is located in a band of 65mm-120mm from flange back (outside of wheel tread centre). The material shelling is more severe close to the tread centre (white dotted line), and cracks with shallow angle are more often in field side of wheel tread (furthest from the flange). During wheel lathe turning, transverse cracks are always propagating downward into wheel, leading to unacceptable material removal, seen Fig. 1(b).

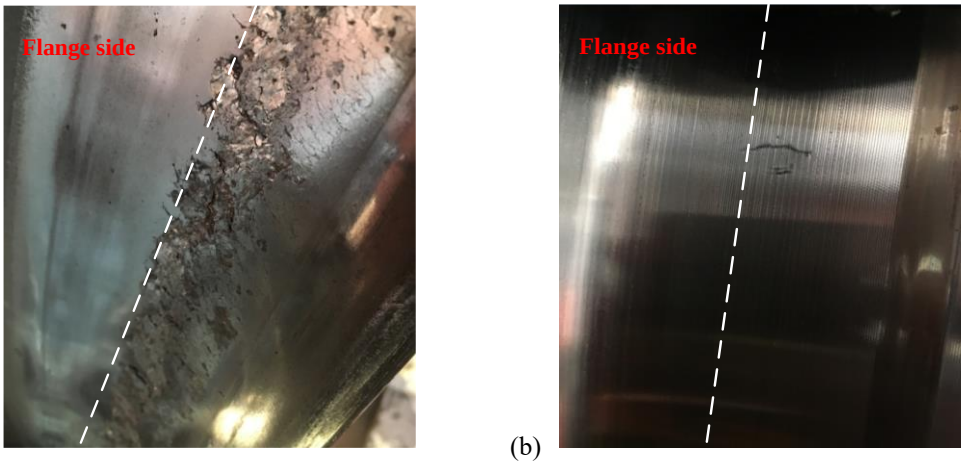

(a) (b)

Fig. 1. Typical damage: (a) surface deterioration, and (b) transverse cracks after wheel turning.

From the observation, the surface damage does not show correlation with the wheelset mounting position, and so do the left and right wheels of a wheelset. However, a distinctive feature of the damage distribution is that the left and right wheels of a same wheelset are rarely observed surface damage together. Fig. 2 gives the typical wheel conditions of left and right wheels on a same wheelset. The surface of left wheel is in well condition whereas the cracks spread around the right wheel surface, and the cracks also located in field side of wheel tread.

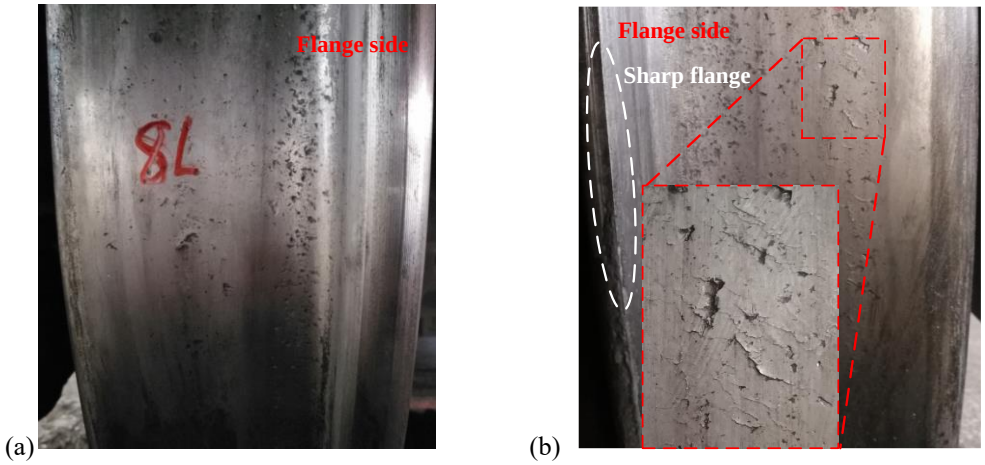

(a) (b)

Fig. 2. Conditions of wheels on a same wheelset: (a) Left wheel, and (b) right wheel with obvious cracks.

Another significant difference of the left and right wheels in Fig. 2 is the flange wear, the flange of right wheel is very sharp (the white dotted ellipse), but the flange of left wheel shows relatively intact. This phenomenon means that severe partial wear is occurring in the wheels, the flange wear of right wheel is quicker than the left. According to the observation, the wheels with severe surface cracks are often accompanied by serious flange wear, but the wheel surface and flange on the other side of wheelset is usually in well condition. To further explore the wear characteristics between left and right wheels, the wheel profiles were measured and compared.

2.2 Wheel profile wear

The wheel profiles were measured at locomotive depot for showing features of wheel wear. Fig. 3(a)

gives measured profiles of a wheelset, which surface conditions is shown in Fig. 2, the right wheel has obvious cracks whereas the left wheel surface is in well condition. It can be found that the values of tread wear and flange wear of right wheel were both higher than the left. For the right wheel, the wear concentrates on a band of 30-100mm from flange back. But for the left wheel, wheel wear most locates on a band of 70-120mm. As a contrast, the profiles of another wheelset in the same locomotive were also measured, as shown in Fig. 3(b). The same shapes of left and right wheel profiles indicate that there is no partial wear occurred, and wheel wear mainly distributes in a band of 40-120mm for both wheels. Field observation also shows that their surface conditions are relatively well and have no apparent cracks.

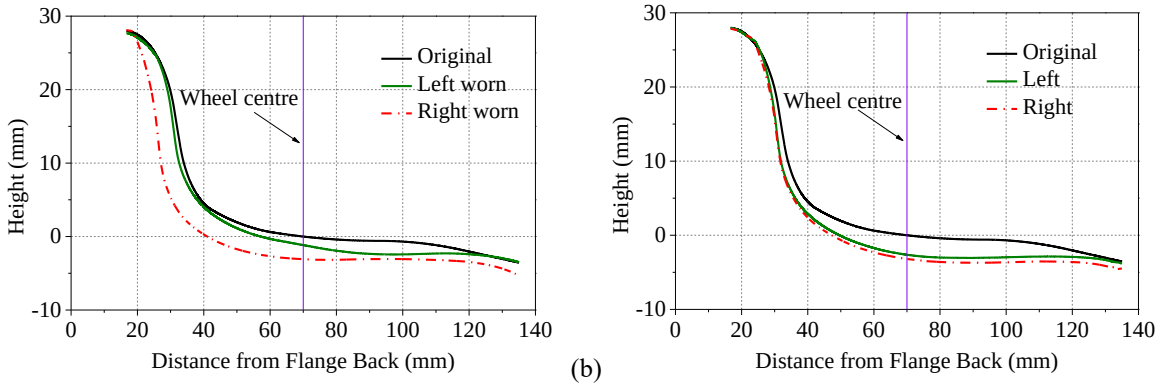

Fig. 3. Measured wheel profiles: (a) With serious surface cracks, and (b) with well surface conditions.

The wheels of 5 locomotives (about 40 wheelsets, 80wheels) were observed and measured successively at locomotive depot, and these locomotives are almost used in the same route. The statistical results show that 7 wheelsets (occurrence rate is 17.5%) suffer obvious partial wear. As observation, the cracks were mainly observed on these 7 wheelsets. It is also clearly found that, only one side wheel of these 7 wheelsets suffers crack damage, also its flange wear and tread wear are higher than the other side wheel. The observed and measured results give evidences that the wheel surface crack has closely correlation with the wheel partial wear. In practical, wheel partial wear is

influenced by so many factors, both from the running route, locomotive aspects and maintenance. After a series of field measurement and survey, the WDD is confirmed to be the main reason of wheel partial wear, and further induces the wheel surface damage. The measured results of the wheel diameter are detail presented as follow.

2.3 Measurements and statistics of WDD

The wheel diameters of all 53 locomotives operating in the fixed line were measured using the ruler of wheel diameter, as shown in Fig. 4(a). The measured position is the center of wheel tread (70mm from flange back). The measured results show that there are 67 wheelsets (occurrence rate is 15.8%) existing obvious WDD (more than 3mm), and these wheelsets are distributed among 35 locomotives, no obvious WDD (less than 3mm) was found in the other 18 locomotives. A total of 17 (occurrence rate is 4.0%) wheelsets have WDD greater than 5mm, which maximum value reaches to 8mm.

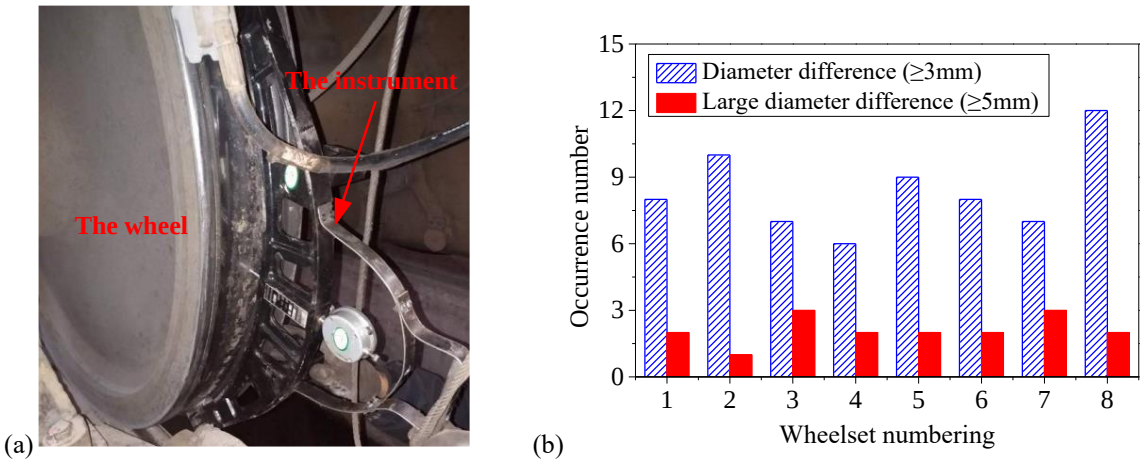

Fig. 4. Measurement of wheel diameter: (a) Measuring ruler, and (b) distribution of WDD.

The occurrence amount of measured WDD in wheelset mounting position is shown in Fig. 4(b). All wheelsets both have possibility to occur WDD, no matter larger than 3mm or 5mm. For the values of WDD more than 3mm, the amount of eighth wheelset is 12, which is slightly higher than others. For WDD more than 5mm, the amounts of third and seventh wheelsets are both 3, and other wheelsets

also have the occurrence.

The statistics of WDD shows that not all locomotives running in the fixed line suffer large WDD, and the WDD occurrence also has no obvious relation with the wheelset mounting position. It can be said that the WDD is not possibly caused by the running route and the locomotive itself.

To further explore the causes of WDD, two locomotives after wheel lathe turning were chosen to measure its wheel diameters, as listed in Table 1. It can be seen that large WDD (larger than 3mm) still exists after wheel turning, which are mainly due to the unqualified maintenance. In the sixth wheelset of locomotive No.1, the value of WDD is 1mm. In the seventh and eighth wheelsets of locomotive No.2, the WDD also reach to 4mm.

Table 1. Diameters (mm) of new turned wheels and its surface conditions after running 10,000km.

Locomotive	**wheelset**	**1**	**2**	**3**	**4**	**5**	**6**	**7**	**8**
No.1	Left	1217	1228	1217	1206	1231	1225	1230	1228
	Right	1215	1228	1216	1208	1231	1231	1229	1231
	WDD	2	0	1	2	0	4	1	3
No.2	Left	1206	1208	1191	1193	1182	1181	1181	1184
	Right	1206	1207	1190	1194	1181	1184	1177	1180
	WDD	0	1	1	1	1	3	4	4

After one month (running about 12,000km) later, the wheel surface conditions of the two chosen locomotives were monitored. The observation shows that, obvious cracks were mainly observed on three wheelset, which are shown by red marks in Table 1. It is clearly found that, the cracks mainly occurred on the wheelset with larger WDD. Fig. 5 gives the wheels' surface condition of these three wheelsets, in which the crack bands are highlighted by red dotted line. For each wheelset, only one side of wheel was observed cracks, but the wheel surface of other side was relatively smooth. And combined Table 1 and Fig. 5, it can be found that, for a wheelset with observed wheel surface cracks, the surface cracks always occurred in wheel with smaller diameter, but the other side wheel with

larger diameter rarely suffered cracks.

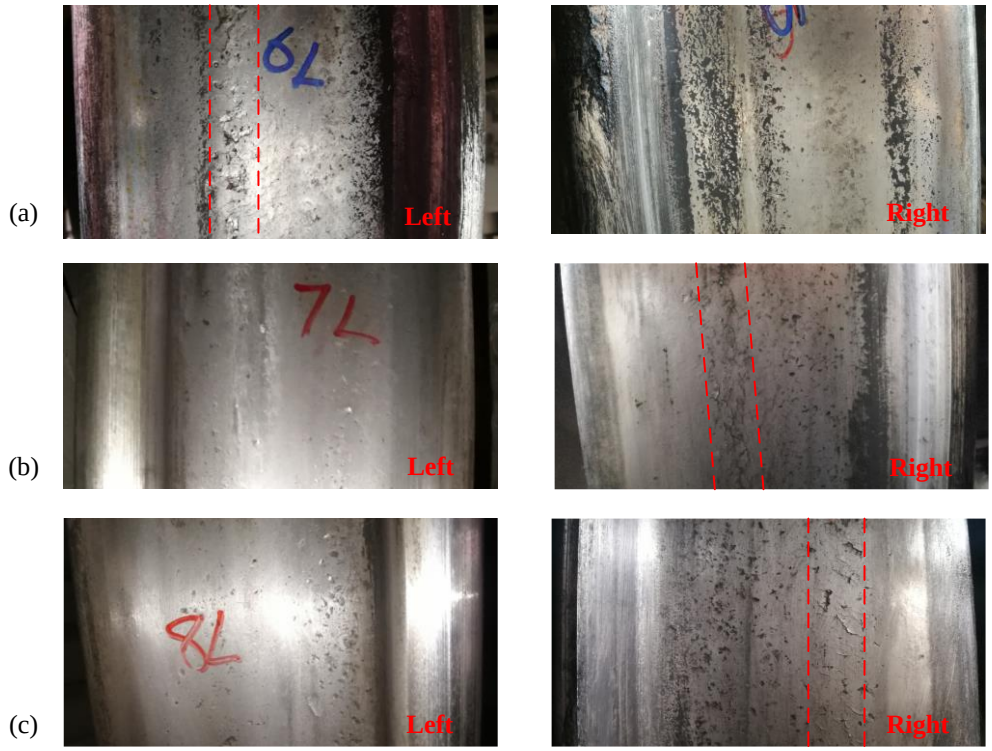

Fig. 5. Wheels with obvious cracks in: (a) sixth wheelset of locomotive No.1, (b) seventh wheelset of locomotive No.2, and (c) eighth wheelset of locomotive No.2

The measurement and observation above indicate that WDD commonly exists in the observed locomotives, which is mainly produced from unqualified maintenance. With large WDD, the partial wear and cracks are developed quickly on wheel tread. The observed cracks are accompanied with two main features: (1) located in the field side of wheel tread, about 65mm-120mm from flange back; (2) occurred in the wheels with smaller diameter, and the smaller wheels also suffer serious partial wear. The observed results are valuable for the following numerical analysis to further investigate the mechanism of wheel surface cracks caused by WDD.

3. Numerical models

Dynamic simulations coupled with RCF prediction models are widely used to analyse the wheel surface cracks and its mitigation measures. In this process, the wheel/rail interaction is firstly

calculated from multi-body dynamic model, and then post processed using RCF predicted model.

3.1. Multi-body dynamic model

The studied locomotive is widely used in Chinese heavy-haul railway, which running speed and traction weight are about 70km/h and 5000t, separately. Each traction unit consists of two identical locomotives connected by coupler system. Each bogie has two motored wheelsets. According to their actual parameters, the dynamic model is developed using the software of SIMPACK, as shown in Fig. 6. Only one dummy freight car is considered in the model to accelerate computing efficiency. The dummy body has only one degree of freedom (longitudinal) to maintain constant speed.

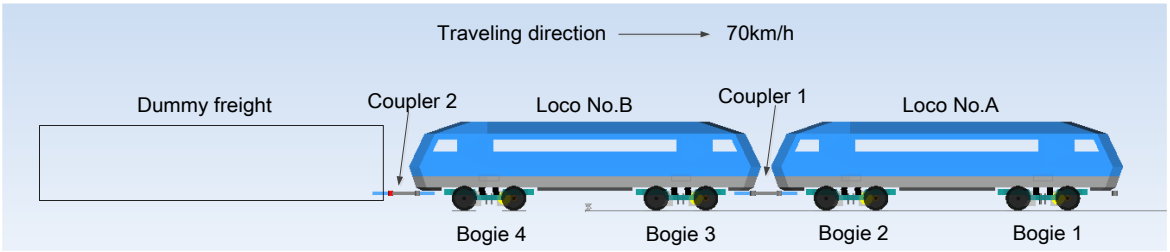

Fig. 6. Locomotive dynamic model.

All wheelsets are equipped with wheel flange lubricating system, which are oil lubricated, as shown in Fig. 7(a). The lubricating system is installed on the bogie, and lubricated oil is sprayed to the flange root automatically in operation. In this condition, the wheel/rail friction of the wheel flange side is different from the field side. When the wheels suffer partial wear and WDD, the wheel/rail contact position is more often located at the flange side. Therefore, the flange lubrication has significant influence on the wheel/rail dynamic interaction, and need to be considered in the simulation. In dynamic model, to simulate flange lubrication, the wheel/rail friction coefficients are set to two values. On the flange side starting from the flange back at 40mm is 0.1 while for the field side is 0.4. The transition length between the two bands is set to 5mm where the friction coefficient changes linearly from 0.1 to 0.4. The setting of wheel/rail friction coefficient is shown in Fig. 7(b).

(a) 

(b) 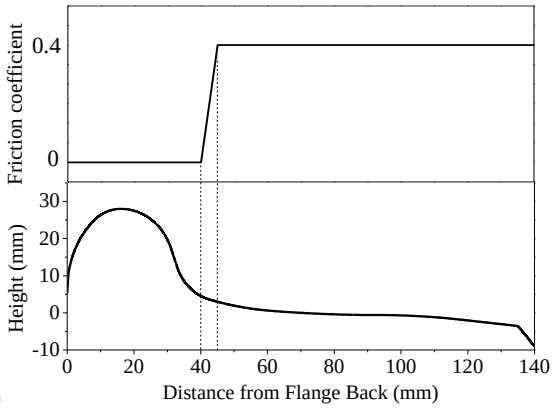

Fig. 7. Wheel flange lubricating system: (a) Installation, and (b) wheel/rail friction coefficient along profile.

The main parameters of locomotive used in model are list in Table 2.

Table 2. Main values of parameters involved in the dynamic model.

Parameters	**Units**	**Values**
Carbody mass	Kg	62600
Bogie mass	Kg	5114
Wheelset mass	Kg	3131
Motor mass	Kg	3662
Wheelset radius	m	0.625
Bogie distance	m	10.06
Wheel base	m	2.6
Free clearance of secondary lateral stopper	mm	20
Elastic clearance of secondary lateral stopper	mm	40
Stiffness of primary suspension along *X* axis	MN/m	166.0e6
Stiffness of primary suspension along *Y* axis	MN/m	58.4e6
Stiffness of primary suspension along *Z* axis	MN/m	1.57e6
Damping of primary suspension along *Z* axis	kN·s/m	45.0e3
Stiffness of secondary suspension along *X* axis	MN/m	0.332e6
Stiffness of secondary suspension along *Y* axis	MN/m	0.332e6
Stiffness of secondary suspension along *Z* axis	MN/m	1.07e6
Damping of secondary suspension along *Y* axis	kN·s/m	39.5e3
Damping of secondary suspension along *Z* axis	kN·s/m	45.0e3

3.2 Predicted model of wheel surface damage

The shakedown map and the damage function ($T\gamma$ model) are commonly used to predict the wheel surface damage, the reliability and accuracy of these two models have been validated in many studies. In the field observation, the wheels with WDD also suffer obvious partial wear, in this condition,

considering the wheel wear is more accurate. Therefore, the damage function is used to predict wheel surface cracks in this paper.

The damage function for wheels was developed from a RCF damage model for rails [14]. The accumulated damage on contact patch is calculated to estimate the degree and location of cracks in wheel profile. Considering the effects of liquid on the propagation of cracks, the cracks damage is only counted when the direction of longitudinal creep forces is opposite to travel direction of wheels, while wear damage is always accumulated. The damage function to predicted wheel RCF and wear is shown in equation (1):

$$T\gamma = T_x\gamma_x + T_y\gamma_y \tag{1}$$

where T is the tangential force and γ is the creepage acting on wheels. The x and y are referring to longitudinal and lateral direction, respectively.

According to the material property of the wheels on the studied locomotives, the values of parameters involved in the predicted model are listed in Table 3. In the predicted results, the positive values mean the crack damage whereas the negative values mean the wear damage.

Table 3. Parameters used in predicted model.

Parameters	Value
Crack initiation threshold	20
Crack rate	3.6×10^{-6}/revolution/N
Wear initiation threshold	100
Wear rate	-5.4×10^{-6}/revolution/N

4. Prediction of wheel surface damage

The locomotive wheels experience a full range of curves, slopes, running speeds, traction and braking forces, or even climatic variation. It is difficult to consider all these factors in dynamic simulation. In this paper the WDD is the key object, therefore, only several conditions including

straight and curved lines are calculated to explain the influence of WDD on wheel surface cracks. In the simulation, the four wheels of bogie 1 (see Fig. 6) were interested and analysed, and the curves were set to right hand.

4.1. Predicted damage without WDD

As a contrast, the wheel surface cracks in different conditions are predicted, as shown in Fig. 8. The running speed was 70km/h and the wheel profile was unworn. It can be found that, for the front bogie, the right wheel of front wheelset and the left wheel of rear wheelset are predicted to suffer crack damage while the others are more likely to suffer wear damage. This paper mainly focuses on the wheel crack damage, therefore, the right wheel of front wheelset and the left wheel of rear wheelset are chosen to analysed. According to the field observation, the crack damage is always found in wheel with smaller diameter and mainly locates in field side of wheel tread. In the following simulation, the smaller values of wheel diameter are set in right wheel of front wheelset and the left wheel of rear wheelset, respectively. The predicted location and value of crack damage happened in these two wheels are analysed in detail.

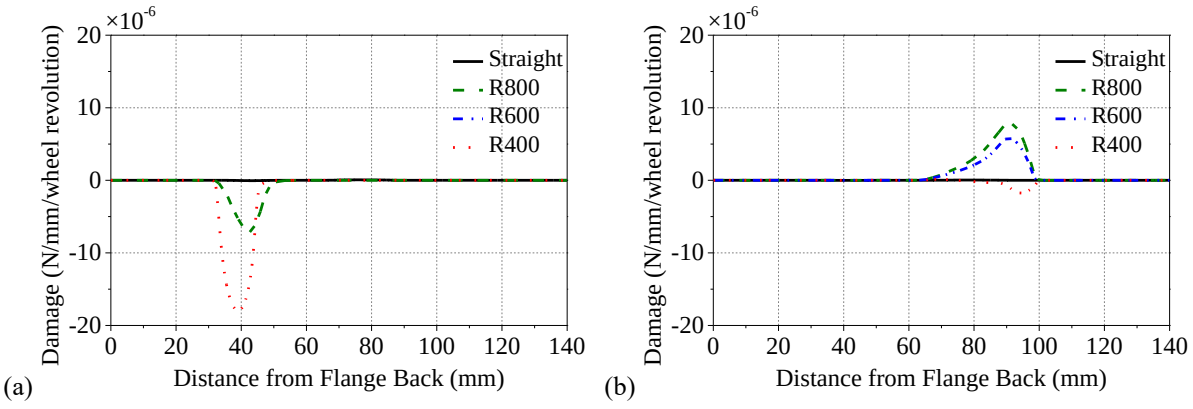

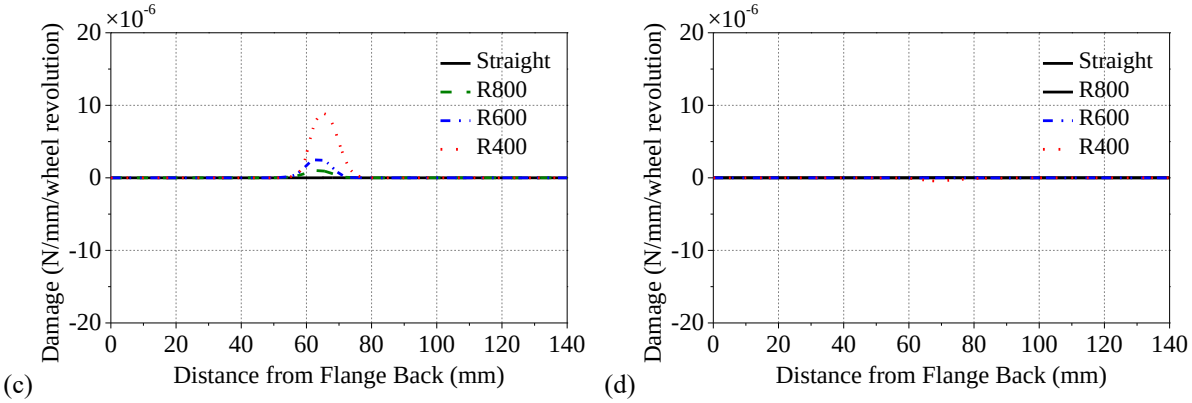

Fig. 8. Predicted crack damage of wheels in a front bogie: (a) left wheel of front wheelset; (b) right wheel of front wheelset; (c) left wheel of rear wheelset; (d) right wheel of rear wheelset.

4.2. Predicted damage with WDD and unworn profile

The variations of location and value of crack damage with the WDD are calculated in this part, the values of WDD are set to 0~8mm and the interval is 2mm. In the simulation, all wheel profiles are unworn and the initial wheel diameters are both 1250mm.

4.2.1 WDD in front wheelset

Fig. 9 gives predicted values of wheel surface damage when the WDD exists in front wheelset, and the right wheel has smaller diameter. It can be found that, with the increase of WDD values, there are no significant increases of crack damage in curves with radius of 800m, 600m, and 400m, whereas the crack damage in straight line increases. Fig. 10 further gives the predicted location of wheel surface damage in straight line. It is clearly found that the location of crack damage moves to flange side with increase of the WDD, which indicates that the cracks are more likely occurring on wheel flange side. However, in field observation, the cracks are observed on outside of wheel centre (about 65-120mm from flange back). The inconsistency of predicted result and observed result is due to the cracks on flange side have more chance to wear off during curving, the measured results (see Fig. 3) and simulated results (see Fig. 8(a)) both give the evidence. Therefore, the WDD existing on front

wheelset with unworn profile does not increase the crack damage significantly in wheel field side.

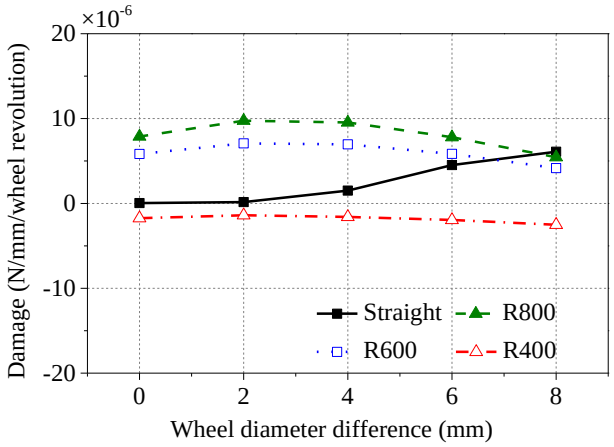

Fig. 9. Variations of wheel surface damage with WDD on front wheelset.

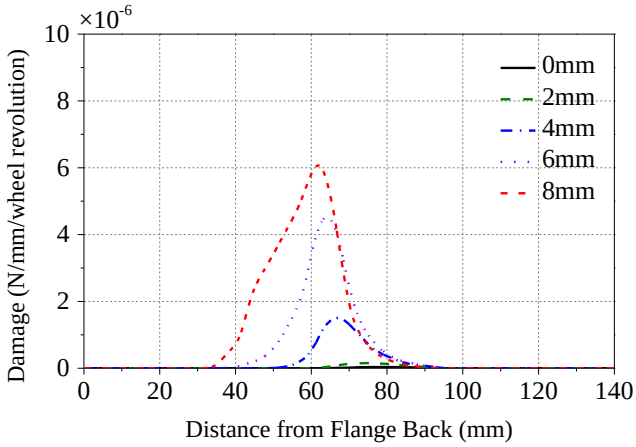

Fig. 10. Variations of damage position with WDD in straight line.

4.2.2 WDD in rear wheelset

Fig. 11 gives predicted values of wheel surface damage when WDD exists on rear wheelset, and the wheel profiles are also unworn. It can be found that, in curves, with the increase of WDD values, the values of crack damage show a tendency of increasing first and then decreasing. And in straight line, the predicted results of crack value are increased. However, the predicted crack damages are also mainly located on the flange side, which are not consistent well with the observation. Fig. 12 gives the predicted locations of crack damage in curve with 800m radius. It can be concluded that, the WDD in rear wheelset with unworn profiles does not increase the crack damage in wheel field side.

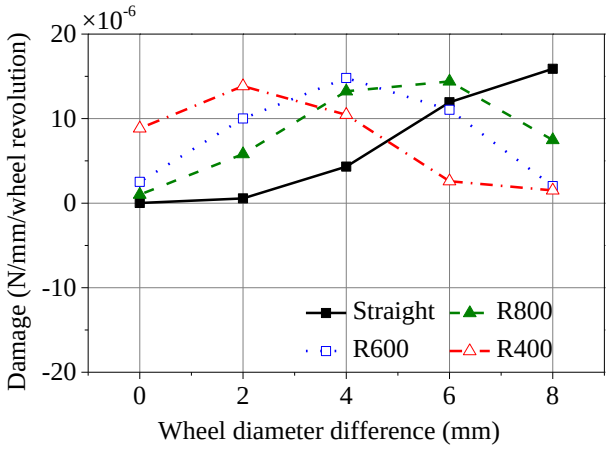

Fig. 11. Variations of wheel surface damage with WDD on rear wheelset.

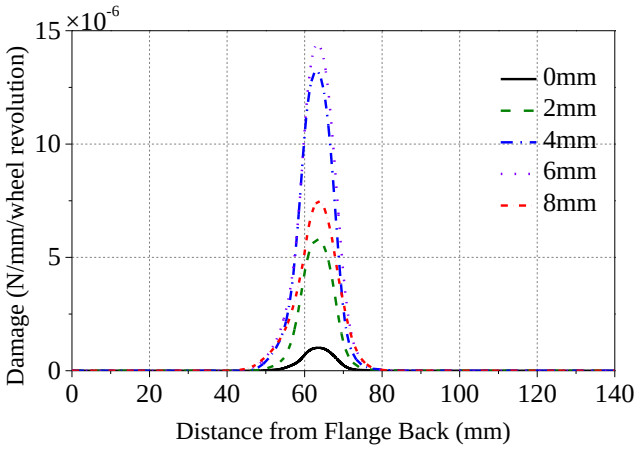

Fig. 12. Variations of damage position with WDD in 800m radius curve.

From the calculated results, the severe cracks on field side of wheel tread (65-120mm from flange back) have less chance to occur when WDD existed in wheelsets with unworn profiles. In another word, only the WDD will not significantly increase the wheel surface cracks located on the field side (see Fig. 2). In the field measurement, another particular phenomenon is the serious wheel partial wear, as described in part 2. This gives an idea that the WDD causes partial wear firstly and further increases the crack damage. Therefore, the measured worn profiles are used in simulation to continue investigating the influence of WDD on surface cracks.

4.3. Predicted damage with WDD and worn profile

As analysed above, the initial WDD will not increase the cracks significantly, but the damage wheel

always accompanied by severe partial wear. In this part, measured wheel profiles and WDD are both used in simulation to further predict the crack damage. The measured profiles are shown in Fig. 3(a), and the measured value of WDD is 8mm. The other wheels use unworn profiles and do not have WDD. It is noted that, for the measured wheelset, its worn profiles and WDD value are confirmed. And in simulation, when the measured wheel profiles are used, its WDD is a certain value.

4.3.1 WDD and worn profiles in front wheelset

When the measured wheel profiles and WDD are set in the front wheelset, the predicted values and locations of crack damage are shown in Fig. 13(a). From the damage position it can be found that the crack damage mainly occurs on the field side of wheel tread (contracted on position of 90-110mm from flange back), which is located in the measured crack band. The comparison between crack damage with and without WDD is given in Fig. 13(b). In condition of WDD and worn profiles, the predicted values of crack damage are much higher than the results without WDD, especially in curves with radius of 600m and 800m. The predicted results mean that with WDD and worn profile, there is significant increase in the wheel surface cracks located on field side of wheel tread, the results show well agreement with the field observation.

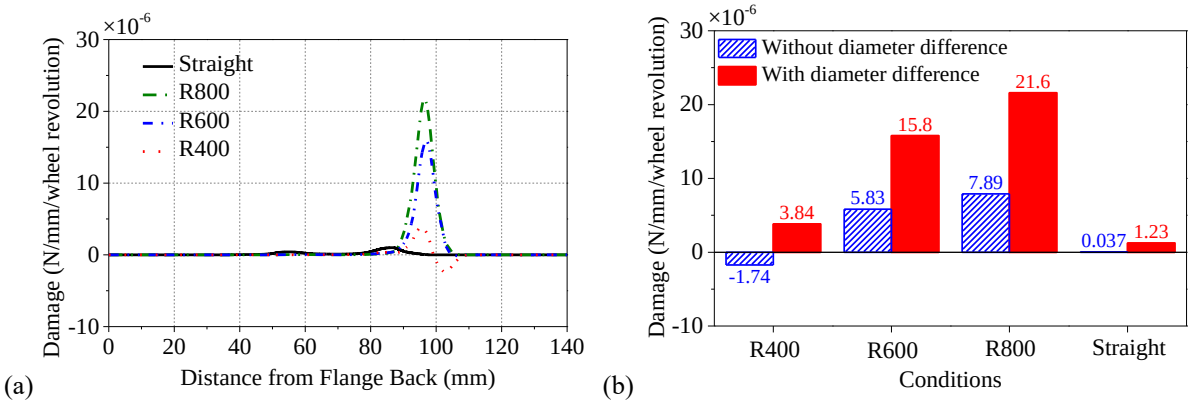

Fig. 13. Predicted result: (a) Damage position with WDD and worn profile in front wheelset; (b) comparison of

crack damage.

4.3.2 WDD and worn profiles in rear wheelset

When WDD and worn profiles set in the rear wheelset, Fig. 14(a) gives the predicted crack position. The crack damage is located on field side of wheel tread (mainly concentrated on about 90mm from flange back) both in straight line and curves, which is coincided with the observed results. Compared with the values of crack damage without WDD, seed Fig. 13(b), the WDD and worn profiles increase the surface cracks significantly, even in the straight line. Although there are predicted crack damage in curves without WDD, the cracks are mainly near wheel centre as shown in Fig. 7(c), which have more chance to worn off in straight line or opposite direction curves. The WDD and worn profiles change the crack location as well as increase the damage values, and in this condition, severe cracks accumulate on wheel surface and eventually cause serious tread spalling.

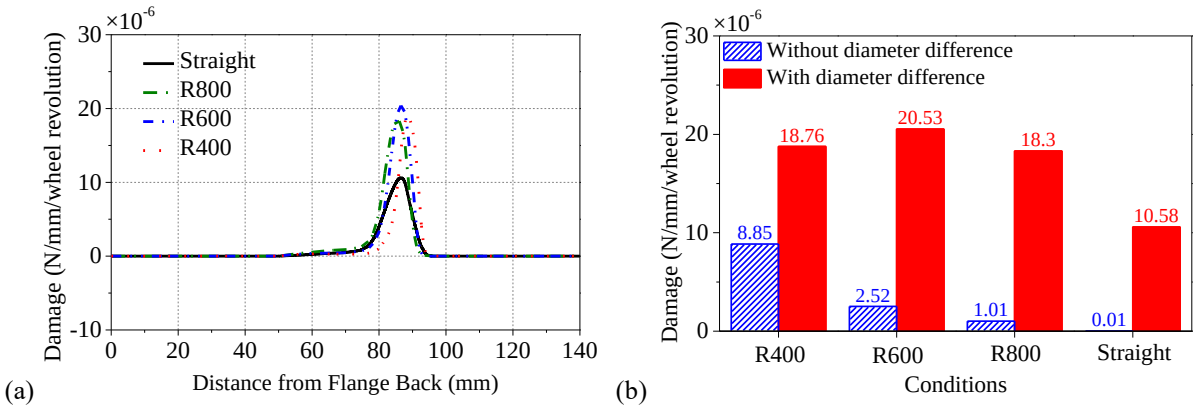

Fig. 14. Predicted result: (a) Damage position with WDD and worn profile in rear wheelset; (b) comparison of crack damage.

From above calculation, it can be found that only the WDD (with unworn profile) will not exacerbate the wheel surface cracks located on field side of wheel tread (about 65-120mm from flange back), no matter for the front or rear wheelsets. However, when the measured worn profiles and value of WDD are set in

simulation, the cracks in field side of tread are increased significantly. The measured profiles show that there are obvious partial wear on left and right wheels in a wheelset, which is mainly caused by the initial WDD from unqualified maintenance. Combined the numerical analysis and field observation, it can be concluded that the initial WDD first causes the wheel partial wear, and the worn profiles combined with WDD further exacerbate wheel surface cracks, especially on position of field side of wheel tread.

The WDD is a critical indicator for the manufacturing and maintenance of railway wheelset, the initial WDD will cause wheel partial wear first, and further exacerbate wheel surface cracks. It is essential to control the values of WDD in practice. For the locomotive in Chinese heavy-haul railway, the executive standard of the threshold of initial WDD is 1mm for a wheelset, 8mm for a bogie, and 20mm for a locomotive, its reliability has been verified by long-term operational service. In practice, large WDD is more likely caused by the wheel maintenance, such as the accuracy of wheel turning lathe. The wheel partial wear is inevitable under the condition of lager WDD. With the increase of running distance, the worn profiles and WDD further increase the surface cracks.

5. Conclusion

Wheel surface crack caused by initial WDD occurring on heavy-haul locomotives is studied based on field observations, statistical analysis, and numerical simulations. The wheel damage features are illustrated, which mainly including the wheel wear and crack location. The mechanism of wheel surface damage caused by initial WDD is studied. Detailed conclusions are drawn as following.

(1) From field observation, the cracks caused by initial WDD are located in a band of 65-120mm from flange back (outside of wheel centre). The cracks not show obvious correlation with axle mounting position.

(2) The measurement of wheel diameter shows that large WDD commonly exists in the locomotive, which maximum value even reaches to 12mm. The new turned wheelset still has a 4mm WDD.

(3) For a wheelset with large initial WDD, the wheel with smaller diameter more likely to suffer crack damage as well as partial wear, whereas the wheel on other side is always in well condition.

(4) Only the initial WDD (with unworn wheel profile) has less chance to increase the surface cracks, especially located in wheel field side. But when the measured worn profiles and WDD are used in simulation, the cracks in field side of wheel tread are increased obviously, which is in accordance with the field observation. Therefore, the initial WDD first causes the wheel partial wear, and the worn profiles combined with the WDD further exacerbate wheel surface cracks.

The features of wheel surface crack as well as wear caused by initial WDD are demonstrated based on field observation and measurement. The mechanism of wheel surface cracks induced by WDD is also clarified based on numerical analysis. Now, to eliminate the initial WDD of the new turned wheelset, the turned process is improved and the wheel diameter of new turned wheel is checked. In this condition, the observation of wheels is being tracked.

Acknowledgements

The authors would like to thank the State Key Laboratory of Traction Power for providing equipment and materials to this project, and the CRRC Datong Electric Locomotive CO., LTD for the cooperation and support. And the authors are grateful to the reviewers for valuable technical advice and help in improving the text of this paper.

Funding

The authors are grateful for the financial support provided by the National Natural Science Foundation of China (Grant No. 51825504, 51735012 and 51605315) and the Program of Introducing Talents of Discipline to Universities (111 Project) (Grant No. B16041), and this paper is also supported by Doctoral Innovation Fund Program of Southwest Jiaotong University.

Conflict of interest

The authors declared that they have no conflicts of interest to this work.

References

[1] Wu Q, Luo S, Xu Z, Ma W. Coupler jackknifing and derailments of locomotives on tangent track. Veh Syst Dyn 2013;51:1784–800. doi:10.1080/00423114.2013.830184.

[2] Ling L, Dhanasekar M, Thambiratnam DP, Sun YQ. Lateral impact derailment mechanisms, simulation and analysis. Int J Impact Eng 2016;94:36–49. doi:10.1016/j.ijimpeng.2016.04.001.

[3] Guo L, Wang K, Chen Z, Shi Z, Lv K, Ji T. Analysis of the car body stability performance after coupler jack-knifing during braking. Veh Syst Dyn 2018;56:900–22. doi:10.1080/00423114.2017.1401099.

[4] Lv K, Wang K, Chen Z, Guo L, Shi Z, Ji T, et al. The effect of the secondary lateral stopper on the compressed stability of the couplers and running safety of the locomotives. Proc Inst Mech Eng Part F J Rail Rapid Transit 2018;232:851–62. doi:10.1177/0954409717699040.

[5] Ekberg A, Åkesson B, Kabo E. Wheel/rail rolling contact fatigue - Probe, predict, prevent. Wear 2014;314:2–12. doi:10.1016/j.wear.2013.12.004.

[6] Ekberg A. Fatigue of railway wheels. Woodhead Publishing Limited; 2009. doi:10.1533/9781845696788.1.211.

[7] Magel EE. Rolling Contact Fatigue: A Comprehensive Review. Fed Railr Adm 2011:132. doi:10.1039/B910216G.

[8] Turnia J, Sinclair J, Perez J. A review of wheel wear and rolling contact fatigue. Proc Inst Mech Eng Part F J Rail Rapid Transit 2007;221:271–89. doi:10.1243/0954409JRRT72.

[9] Dirks B, Enblom R, Berg M. Prediction of wheel profile wear and crack growth – comparisons with measurements. Wear 2016;366–367:84–94. doi:10.1016/j.wear.2016.06.026.

[10] Hossein-Nia S, Sichani MS, Stichel S, Casanueva C. Wheel life prediction model–an alternative to the FASTSIM algorithm for RCF. Veh Syst Dyn 2018;56:1051–71. doi:10.1080/00423114.2017.1403636.

[11] Hossein Nia S, Casanueva C, Stichel S. Prediction of RCF and wear evolution of iron-ore locomotive wheels. Wear 2015;338–339:62–72. doi:10.1016/j.wear.2015.05.015.

[12] Mazzù A, Donzella G. A model for predicting plastic strain and surface cracks at steady-state wear and ratcheting regime. Wear 2018;400–401:127–36. doi:10.1016/j.wear.2018.01.002.

[13] Grassie SL. The strength of surfaces in rolling contact 1989. doi:10.1243/PIME.

[14] Tunna J, Sinclair J PJ. Research Programme. London: 2007. doi:10.1007/978-3-642-31641-8_3.

[15] Fletcher DI, Beynon JH. The effect of intermittent lubrication on the fatigue life of pearlitic rail steel in rolling-sliding contact. Proc Inst Mech Eng Part F J Rail Rapid Transit

2002;214:145–58. doi:10.1243/0954409001531270.

[16] Liu W, Ma W, Luo S, Zhu S, Wei C. Research into the problem of wheel tread spalling caused by wheelset longitudinal vibration. Veh Syst Dyn 2015;53:546–67. doi:10.1080/00423114.2015.1008015.

[17] Stichel S, Mohr H, Ågren J, Enblom R. Investigation of the risk for rolling contact fatigue on wheels of different passenger trains. Veh Syst Dyn 2008;46:317–27. doi:10.1080/00423110801939188.

[18] Ekberg A, Kabo E, Karttunen K, Lindqvist B, Lundén R, Nordmark T, et al. Identifying the root causes of damage on the wheels of heavy haul locomotives and its mitigation. Proc Inst Mech Eng Part F J Rail Rapid Transit 2014;228:663–72. doi:10.1177/0954409714526165.

[19] Spangenberg U, Fröhling RD, Els PS. Long-term wear and rolling contact fatigue behaviour of a conformal wheel profile designed for large radius curves. Veh Syst Dyn 2019;57:44–63. doi:10.1080/00423114.2018.1447677.

[20] Fröhling R, Spangenberg U, Hettasch G. Wheel/rail contact geometry assessment to limit rolling contact fatigue initiation at high axle loads. Veh Syst Dyn 2012;50:319–34. doi:10.1080/00423114.2012.665163.

[21] Shevtsov IY, Markine VL, Esveld C. Design of railway wheel profile taking into account rolling contact fatigue and wear. Wear 2008;265:1273–82. doi:10.1016/j.wear.2008.03.018.

[22] Spangenberg U, Fröhling RD, Els PS. Influence of wheel and rail profile shape on the initiation of rolling contact fatigue cracks at high axle loads. Veh Syst Dyn 2016;54:638–52. doi:10.1080/00423114.2016.1150496.

[23] Spangenberg U, Fröhling RD, Els PS. The effect of rolling contact fatigue mitigation measures on wheel wear and rail fatigue. Wear 2018;398–399:56–68. doi:10.1016/j.wear.2017.11.012.

[24] Makino T, Kato T, Hirakawa K. The effect of slip ratio on the rolling contact fatigue property of railway wheel steel. Int J Fatigue 2012;36:68–79. doi:10.1016/j.ijfatigue.2011.08.014.

[25] Zhu WT, Guo LC, Shi LB, Cai ZB, Li QL, Liu QY, et al. Wear and damage transitions of two kinds of wheel materials in the rolling-sliding contact. Wear 2018;398–399:79–89. doi:10.1016/j.wear.2017.11.023.

[26] Seo JW, Jun HK, Kwon SJ, Lee DH. Rolling contact fatigue and wear of two different rail steels under rolling-sliding contact. Int J Fatigue 2016;83:184–94. doi:10.1016/j.ijfatigue.2015.10.012.

[27] Molyneux-Berry P, Bevan A. Wheel surface damage: Relating the position and angle of forces to the observed damage patterns. Veh Syst Dyn 2012;50:335–47. doi:10.1080/00423114.2012.665164.

[28] Zhao X, Wen Z, Liu D, Liu C, Zhao X. Observations and monitoring of the rolling contact fatigue of Chinese high speed wheels. Proc 2016 IEEE Int Wheel Congr IWC 2016 2017:55–9. doi:10.1109/IWC.2016.8068367.

[29] Zhao X, An B, Zhao X, Wen Z, Jin X. Local rolling contact fatigue and indentations on high-speed railway wheels: Observations and numerical simulations. Int J Fatigue 2017;103:5–16. doi:10.1016/j.ijfatigue.2017.05.014.

[30] Deuce R, Ekberg A, Kabo E. Mechanical deterioration of wheels and rails under winter

conditions – mechanisms and consequences. Proc Inst Mech Eng Part F J Rail Rapid Transit 2018;0:1–9. doi:10.1177/0954409718802437.